

**$(t, p)$  reactions on  ${}^4\text{He}$ ,  ${}^6\text{Li}$ ,  ${}^7\text{Li}$ ,  ${}^9\text{Be}$ ,  ${}^{10}\text{B}$ ,  ${}^{11}\text{B}$ , and  ${}^{12}\text{C}^\dagger$** 

F. Ajzenberg-Selove\*

*Department of Physics, University of Pennsylvania, Philadelphia, Pennsylvania 19104  
and University of California, Los Alamos Scientific Laboratory, Los Alamos, New Mexico 87545*

E. R. Flynn and Ole Hansen†

*University of California, Los Alamos Scientific Laboratory, Los Alamos, New Mexico 87545*

(Received 13 December 1977)

A study of the  $(t, p)$  reactions on  ${}^4\text{He}$ ,  ${}^6\text{Li}$ ,  ${}^7\text{Li}$ ,  ${}^9\text{Be}$ ,  ${}^{10}\text{B}$ ,  ${}^{11}\text{B}$ , and  ${}^{12}\text{C}$  has been carried out using 23 MeV tritons and an Elbek-type spectrograph using photographic emulsions as detectors. A total of 71 states of  ${}^6\text{He}$ ,  ${}^8\text{Li}$ ,  ${}^9\text{Li}$ ,  ${}^{11}\text{Be}$ ,  ${}^{12}\text{B}$ ,  ${}^{13}\text{B}$ , and  ${}^{14}\text{C}$  have been studied. Some of the states had not been previously reported. In other cases new values of excitation energies and widths are proposed. Attempts have been made to fit the 62 angular distributions we obtained with the distorted-wave Born approximation: no systematic analysis was possible except in the case of  $L = 0$  distributions.

[NUCLEAR REACTIONS  ${}^4\text{He}$ ,  ${}^6\text{Li}$ ,  ${}^7\text{Li}$ ,  ${}^9\text{Be}$ ,  ${}^{10}\text{B}$ ,  ${}^{11}\text{B}$ ,  ${}^{12}\text{C}(t, p)$ ,  $E = 23$  MeV; measured  $\sigma(\theta)$ .  ${}^6\text{He}$ ,  ${}^8\text{Li}$ ,  ${}^9\text{Li}$ ,  ${}^{11}\text{Be}$ ,  ${}^{12}\text{B}$ ,  ${}^{13}\text{B}$ ,  ${}^{14}\text{C}$  deduced levels,  $J^\pi$ ,  $\Gamma_{\text{c.m.}}$ .]

## I. INTRODUCTION

Since the pioneering work of Middleton *et al.*<sup>1,2</sup> in studying  $(t, p)$  reactions on light nuclei at  $E_t = 6$  to 14 MeV and analyzing them by PWBA (plane-wave Born approximation), there have been only a few attempts to study neutron rich light nuclei using the  $(t, p)$  reaction because of the relative lack of high energy triton beams. Stokes and Young<sup>3,4</sup> have studied the  $(t, p)$  reactions on  ${}^4\text{He}$  and on  ${}^7\text{Li}$  at  $E_t = 22$  and 15 MeV, respectively, and Ajzenberg-Selove *et al.*<sup>5</sup> have reported on the  ${}^9\text{Be}(t, p){}^{11}\text{Be}$  reaction at  $E_t = 20$  MeV. The present experiment was undertaken<sup>6</sup> to study the  $(t, p)$  reaction on all the stable nuclei between  $A = 4$  and  $A = 12$ , to see if the angular distributions of the protons could be analyzed so as to provide information on the parameters of the states in the final nuclei and to determine if new states in  ${}^6\text{He}$ ,  ${}^8\text{Li}$ ,  ${}^9\text{Li}$ ,  ${}^{11}\text{Be}$ ,  ${}^{12}\text{B}$ ,  ${}^{13}\text{B}$ , and  ${}^{14}\text{C}$  could be observed at the higher excitation energies that were permitted by the availability of 23 MeV tritons.

## II. EXPERIMENTAL PROCEDURES AND RESULTS

A beam of 23 MeV tritons was obtained from the Los Alamos three-stage Van de Graaff facility. The reaction products were momentum analyzed in a broad range spectrograph and detected in nuclear emulsions placed along the focal plane. The emulsions were covered with Al foils thick enough to stop all impinging charged particles other than protons. The parameters of the runs are displayed in Table I. The energy resolution was, typically 20 keV full width at half maximum.

A.  ${}^4\text{He}(t, p){}^6\text{He}$ 

Only two states have been clearly established<sup>7</sup> in  ${}^6\text{He}$ : the bound ground state, which decays by  $\beta^-$  emission to  ${}^6\text{Li}_{\text{g.s.}}$ , and an unbound excited state at  $1.797 \pm 0.025$  MeV ( $\Gamma_{\text{c.m.}} = 113 \pm 20$  keV)<sup>7</sup> (see Table II). Figure 1 shows the spectrum of the protons to these two states at  $\theta = 10^\circ$  and Fig. 2 shows the angular distributions of the two proton groups, which should be characteristic of  $L = 0$  and 2. The shape of the angular distributions agree with those reported by Stokes and Young<sup>3</sup> in the  $(t, p)$  reaction at  $E_t = 22$  MeV but the absolute differential cross sections we report are a factor of 2 lower than in the earlier study. Attempts by Stokes and Young<sup>3</sup> to fit the angular distributions theoretically were not successful. (We will comment on the  $L = 0$  distribution in Sec. II H.) The absolute cross sections were obtained from the known gas cell geometry<sup>8</sup> and the gas pressure.

B.  ${}^6\text{Li}(t, p){}^8\text{Li}$ 

Five relatively sharp states have been reported<sup>7,9</sup> in  ${}^8\text{Li}$ : the two bound states at 0 and 0.981 MeV with  $J^\pi = 2^+$  and  $1^+$ , the  $3^+$  state at 2.621 MeV ( $\Gamma_{\text{c.m.}} = 31 \pm 5$  keV), a state of unknown  $J^\pi$  at 6.53 MeV ( $\Gamma_{\text{c.m.}} < 40$  keV), and the first  $T = 2$  state<sup>9</sup> at 10.82 MeV ( $J^\pi = 0^+$ ). We observe the four  $T = 1$  states (Fig. 3) and our values for the widths of  ${}^8\text{Li}^*(2.26, 6.53)$  are in good agreement with the previous values: see Table II. We do not observe the  $T = 2$  state at the three angles at which we scanned in the relevant  $E_x$  region ( $\theta = 5.5^\circ, 35^\circ, \text{ and } 45^\circ$ ) (excitation of a  $T = 2$  state is "forbidden" by isospin

TABLE I. Parameters of runs.

Target	Kind	Enrichment <sup>d</sup>	Thickness or pressure	$B^a$ (kG)	$\theta_{\text{lab}}$ (deg)	Charge <sup>b</sup> ( $\mu\text{C}$ )	$Q_m^c$ (keV)
$^4\text{He}$	Gas <sup>e</sup>	...	39 Torr	5.00	7.5-55	600-1800	-7511 $\pm$ 3.5
$^6\text{Li}$	On 40 $\mu\text{g}/\text{cm}^2$ C	99.32%	50 $\mu\text{g}/\text{cm}^2$ <sup>f</sup>	6.83	5.4-85	1200	801 $\pm$ 1.2
$^7\text{Li}$	On 40 $\mu\text{g}/\text{cm}^2$ C	99.9%	50 $\mu\text{g}/\text{cm}^2$ <sup>f</sup>	6.30	5.5-55	300-1200	-2386 $\pm$ 2.2
$^9\text{Be}$	Self-supported	...	60 $\mu\text{g}/\text{cm}^2$	6.83	5.4-55	600-900	-1167 $\pm$ 6
$^{10}\text{B}$	Self-supported	96.5%	50 $\mu\text{g}/\text{cm}^2$ <sup>f</sup>	7.79	5.5-55	600-1500	6342 $\pm$ 1.3
$^{11}\text{B}$	Self-supported	98.1%	85 $\mu\text{g}/\text{cm}^2$ <sup>f</sup>	6.83	5.5-55	300-1500	-233 $\pm$ 4
$^{12}\text{C}$	Self-supported	Isotopic	150 $\mu\text{g}/\text{cm}^2$ <sup>f</sup>	7.55	5.5-55	60-300	4641.0 $\pm$ 0.1
$^{12}\text{C}$	Methane gas <sup>e</sup>	Isotopic	39.5 Torr	7.55	7.5, 15, 55	600-1200	4641.0 $\pm$ 0.1

<sup>a</sup> Magnetic field of the spectrograph.

<sup>b</sup> Range of incident charge; the higher charges were used at the larger angles.

<sup>c</sup> For the  $(t, p)$  reaction on the target nucleus using the masses of A. H. Wapstra and K. Bos, At. Data Nucl. Data Tables 19, 175 (1977).

<sup>d</sup> Enriched isotopes were obtained from the Stable Isotopes Division of ORNL.

<sup>e</sup> For a description of the gas cell see Ref. 8.

<sup>f</sup> Nominal thickness.

TABLE II. Parameters of some states observed in the  $(t, p)$  reactions in  $^4\text{He}$ ,  $^6\text{Li}$ ,  $^7\text{Li}$ , and  $^9\text{Be}$ .

State in	$E_x^a$ (MeV)	$J^\pi^a$	$L^d$	$(d\sigma/d\Omega)_{\text{c.m.}}^{\text{max } b}$ (mb/sr)	$I_{\text{c.m.}}^{b,c}$	$\Gamma_{\text{c.m.}}^b$ (keV)
$^6\text{He}^e$	0	$0^+$	0	$0.91 \pm 0.02$		
	1.80	$2^+$	2	$4.16 \pm 0.04$		
$^8\text{Li}^f$	0	$2^+$	2		$\equiv 1$	
	0.981	$1^+$	0		0.6	
	2.261	$3^+$	2		1.9	$35 \pm 10$
	$6.54 \pm 0.03^b$	$\geq 4^b$	$\geq 4^b$		0.2	$35 \pm 15$
$^9\text{Li}^g$	0	$\frac{3}{2}^-^b$	$0^b$		$\equiv 1$	
	2.69	$(\frac{1}{2}^-)$			0.2	
	$4.31 \pm 0.020^b$		$(1)^b$		2.4	$100 \pm 30$
	$6.435 \pm 0.020^b$	$\geq \frac{3}{2}^b$	$\geq 4^b$		0.4	$40 \pm 20$
$^{11}\text{Be}^h$	0	$\frac{1}{2}^+$	1	$0.16 \pm 0.01$		
	$0.318 \pm 0.010^b$	$\frac{3}{2}^-$	2	$0.59 \pm 0.02$		
	$1.764 \pm 0.020^b$	$(\frac{1}{2}, \frac{3}{2}, \frac{5}{2})^+$	1	$1.57 \pm 0.02$		
	$3.877 \pm 0.030^b$	$\geq \frac{1}{2}^+$	$\geq 3^b$	$0.13 \pm 0.01$		
	$3.943 \pm 0.030^b$	$\frac{3}{2}^-^b$	$0^b$	$1.08 \pm 0.02$		
	$5.231 \pm 0.030^b$			$2.03 \pm 0.04$		
	$6.69 \pm 0.030^b$			$1.69 \pm 0.03$		
	$8.80 \pm 0.04^b$			$3.03 \pm 0.05$		
	$10.59 \pm 0.05^b$					$210 \pm 40$

<sup>a</sup> F. Ajzenberg-Selove and T. Lauritsen, Nucl. Phys. A227, 1 (1974); F. Ajzenberg-Selove, *ibid.* A248, 1 (1975). See also the discussion in the text.

<sup>b</sup> From this work. Uncertainties shown in  $(d\sigma/d\Omega)$  are statistical only. We estimate the absolute uncertainties to be  $\pm 20\%$ .

<sup>c</sup> Relative intensities in the center-of-mass system at  $\theta_{\text{lab}} = 25^\circ$  ( $^8\text{Li}$ ) and  $15^\circ$  ( $^9\text{Li}$ ).

<sup>d</sup> Based on  $J^\pi$  shown in column three, except where indicated otherwise.

<sup>e</sup> See Figs. 1 and 2.

<sup>f</sup> See Figs. 3 and 4.

<sup>g</sup> See Figs. 5 and 6.

<sup>h</sup> See Fig. 1 in F. Ajzenberg-Selove, R. F. Casten, O. Hansen, and T. J. Mulligan, Phys. Lett. 40B, 205 (1972), and Fig. 7 here.

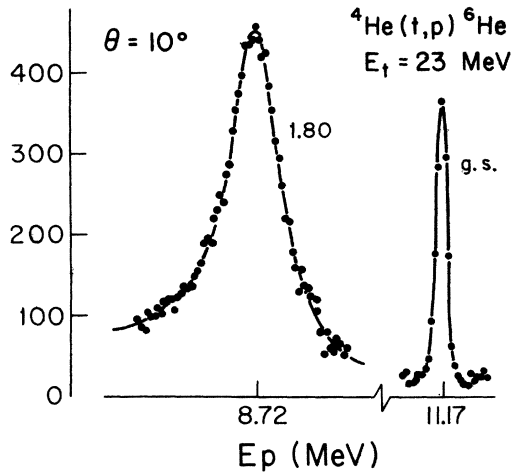


FIG. 1. Spectrum of the protons from the  ${}^4\text{He}(t,p){}^6\text{He}$  reaction at  $\theta_{\text{lab}} = 10^\circ$ . The ordinate shows the average number of protons counted in a  $250 \mu\text{m}$  wide swath of the emulsion.

conservation), nor do we observe any other states of  ${}^8\text{Li}$  with  $\Gamma \leq 100 \text{ keV}$  below  $E_x = 10.8 \text{ MeV}$  at those three angles and below  $E_x = 7 \text{ MeV}$  at the other angles of observation.

The angular distributions we observe for the protons to  ${}^8\text{Li}^*(0, 0.98, 2.26, 6.53)$  are shown in

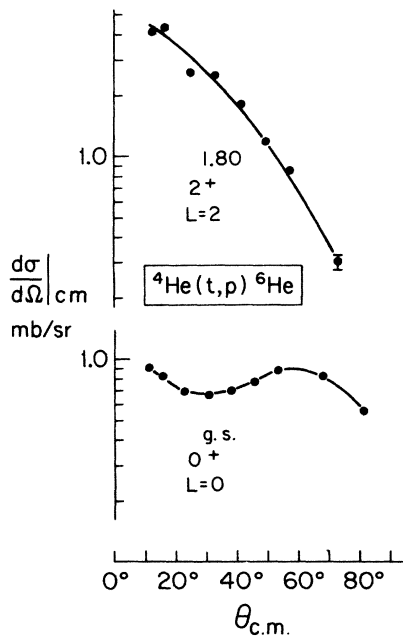


FIG. 2. Angular distributions of the protons to  ${}^6\text{He}^*(0, 1.80)$ . The  $L$  values shown are determined from  $J^\pi$  known from previous work. The error bars reflect statistical errors only. The absolute differential cross sections are estimated to be known to  $\pm 20\%$ . The lines through the data are not theoretical fits.

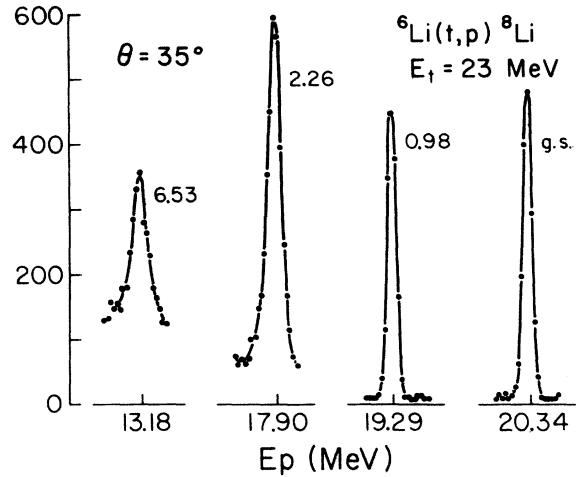


FIG. 3. Spectrum of the protons from  ${}^6\text{Li}(t,p){}^8\text{Li}$  at  $\theta = 35^\circ$ . See also the caption to Fig. 1.

Fig. 4. The distributions to  ${}^8\text{Li}_{\text{g.s.}}$  and to  ${}^8\text{Li}^*(2.26)$  should both be characteristic of  $L=2$  but the latter state is unbound, although only by  $0.23 \text{ MeV}$ : The "total" cross section ( $\theta_{\text{c.m.}} < 90^\circ$ ) for this  $3^+$  state is greater than that to the  $2^+$  ground state by a factor of 1.7. The intensity of the proton groups to the state of unknown  $J^\pi$  at  $E_x = 6.53 \text{ MeV}$  at forward

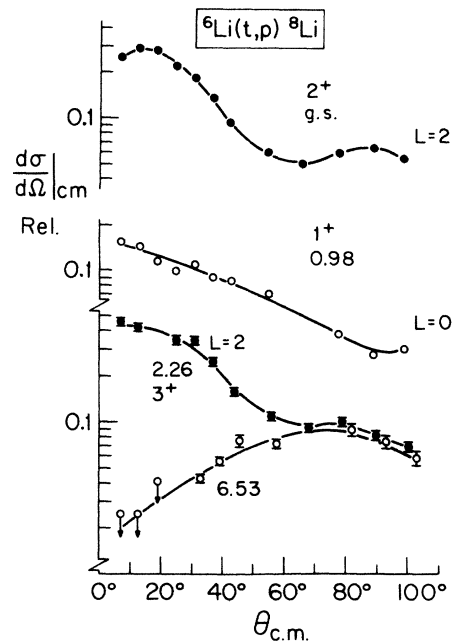


FIG. 4. Angular distributions of the protons to  ${}^8\text{Li}^*(0, 0.98, 2.26, 6.53)$ . The  $L$  values shown are determined from  $J^\pi$  known from previous work. The target thickness was nominal and only the relative differential cross sections can be shown. The error bars show statistical uncertainties only.

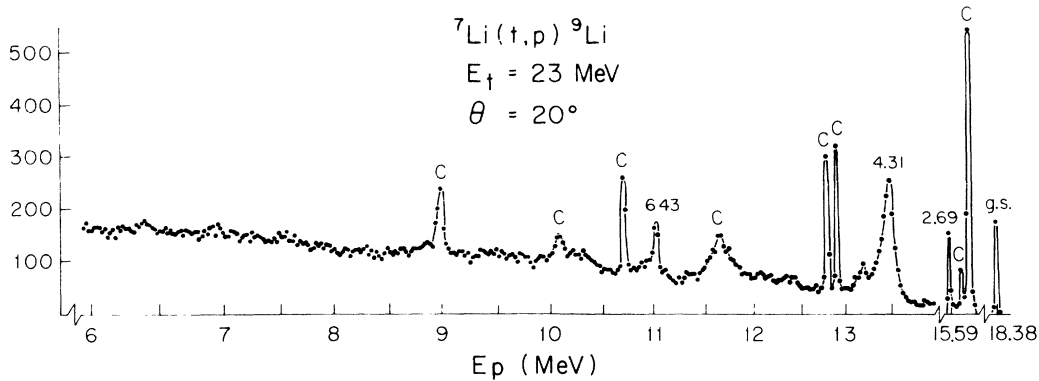


FIG. 5. Spectrum of the protons from  ${}^7\text{Li}(t,p){}^9\text{Li}$  at  $\theta = 20^\circ$ . See also the caption to Fig. 1. Groups labeled C are due to the  ${}^{12}\text{C}(t,p){}^{14}\text{C}$  reaction.

angles is very low which is indicative of  $L > 3$ . The angular distribution is in fact similar to that of the protons to  ${}^{12}\text{B}^*(2.72)$  (see Sec. IID and Fig. 9) which is  $L = 4$ . Therefore we suggest that  $L \geq 4$  for the transition to  ${}^9\text{Li}^*(6.53)$ . If  $L = 4$ ,  $J^\pi = 4^+$  or  $5^+$ ; while if  $L = 5$ ,  $J^\pi = 5^+$  or  $6^+$ . Thus the  $J$  of  ${}^9\text{Li}^*(6.53)$  is  $\geq 4$ , which would also be consistent with its small width despite the fact that it is unbound via several channels. The analog regions in  ${}^8\text{Be}$  and  ${}^8\text{B}$  are not well enough known to permit comparisons to be made.

### C. ${}^7\text{Li}(t,p){}^9\text{Li}$

Four relatively sharp states have been reported<sup>4,7</sup> in  ${}^9\text{Li}$ : the two bound states at 0 and 2.691 MeV with  $J^\pi = (\frac{3}{2})^-$  and  $(\frac{1}{2})^-$ , and two neutron-unbound

states of unknown  $J^\pi$  at  $E_x = 4.31 \pm 0.03$  and  $6.41 \pm 0.02$  MeV ( $\Gamma_{\text{c.m.}} = 250 \pm 30$  keV and  $< 100$  keV). In addition, a state has been reported at  $E_x = 5.38 \pm 0.06$  MeV with  $\Gamma_{\text{c.m.}} = 0.6 \pm 0.1$  MeV. Figure 5 shows one of our spectra: we clearly observe  ${}^9\text{Li}^*(0, 2.69, 4.31, 6.41)$ . The broader state at 5.38 MeV is not seen as a separate group but its existence is not inconsistent with our data. We observe no other sharp states ( $\Gamma \leq 0.2$  MeV) of  ${}^9\text{Li}$  up to  $E_x = 12$  MeV at  $\theta = 20^\circ, 25^\circ$ , and  $30^\circ$  assuming a reasonable population for such states. The groups labeled C in Fig. 5 are from known states in  ${}^{14}\text{C}$  and are due to the carbon backing of the  ${}^7\text{Li}$  target. The widths we report for  ${}^9\text{Li}^*(4.31, 6.41)$  are considerably less than those reported ( $250 \pm 30, < 100$  keV) in the earlier<sup>4</sup>  $(t,p)$  work: We report  $100 \pm 30$  and  $40 \pm 20$  keV, respectively.

Young and Stokes<sup>4</sup> have reported angular distri-

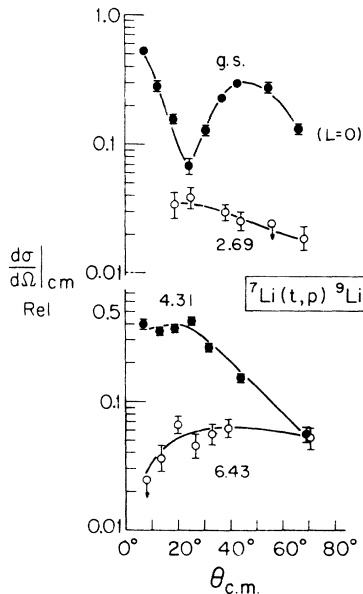


FIG. 6. Angular distributions of the protons to  ${}^9\text{Li}^*(0, 2.69, 4.31, 6.43)$ . See also the caption to Fig. 4.

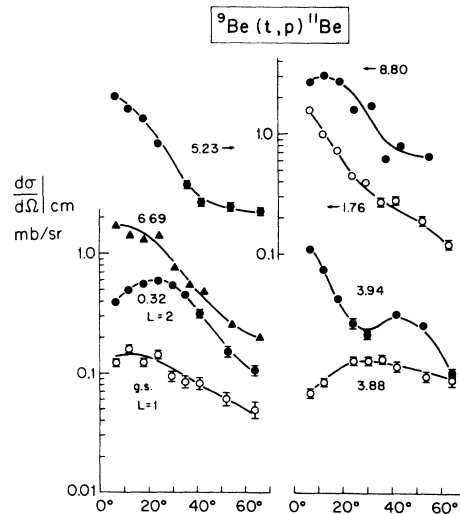


FIG. 7. Angular distributions of the protons to  ${}^{11}\text{Be}^*(0, 0.32, 1.76, 3.88, 3.94, 5.23, 6.69, 8.80)$ . See also the caption to Fig. 2.

TABLE III. Optical model parameters. The triton parameters are the same in optical model 1 (OM1) and OM2; the asterisk indicates a derivative form.

		$V_r$ (MeV)	$r_r$ (fm)	$a_r$ (fm)	$W_I$ (MeV)	$r_I$ (fm)	$a_I$ (fm)	$W_{s.o.}$ (MeV)	$r_{s.o.}$ (fm)	$a_{s.o.}$ (fm)
OM1	Triton	174	1.14	0.49	19.4	1.53	1.07			
	Proton	49	1.14	0.61	6.4*	1.14	0.62	6.3	1.14	0.62
OM2	Proton	53	1.24	0.63	10.4*	1.38	0.32	4.9	1.20	0.31

butions of the protons to  ${}^9\text{Li}^*(0, 4.31, 6.41)$  at  $E_t = 15$  MeV. The angular distributions we present for these three states and only partially because of contamination problems, for  ${}^9\text{Li}^*(2.69)$  are shown in Fig. 6. At  $E_t = 23$  MeV the shapes of the distributions are consistent with those in the earlier study.<sup>4</sup> The angular distribution of the protons to  ${}^9\text{Li}(0)$  is characteristic of  $L=0$  (see Sec. II H); that for  ${}^9\text{Li}^*(6.43)$  is characteristic of  $L \geq 4$  (see Sec. II B). The identification of the distribution for  ${}^9\text{Li}^*(4.31)$  is less certain but it appears to be characteristic of  $L=1$  or 2 with the former preferred by comparison with Fig. 7, for instance.

#### D. ${}^9\text{Be}(t, p) {}^{11}\text{Be}$

We observe the same states in  ${}^{11}\text{Be}$  reported in a previous experiment<sup>5</sup> at  $E_x = 20$  MeV, and one additional one at  $E_x = 10.62 \pm 0.08$  MeV ( $\Gamma_{\text{c.m.}} = 210 \pm 40$  keV): see Table II. Angular distributions are displayed in Fig. 7 for the protons to  ${}^{11}\text{Be}^*(0, 0.32, 1.76, 3.88, 3.94, 5.23, 6.69, 8.80)$ .  ${}^{11}\text{Be}^*(0, 0.32)$  have<sup>10</sup>  $J^\pi = \frac{1}{2}^+$  and  $\frac{1}{2}^-$  and should be reached by  $L=1$  and 2, respectively. An earlier  $(t, p)$  experiment<sup>1</sup> at  $E_t = 14.0$  MeV suggested  $L=1$  and therefore  $J^\pi = (\frac{1}{2}, \frac{3}{2}, \frac{5}{2})^+$  for  ${}^{11}\text{Be}^*(1.78)$ : its analog state in  ${}^{11}\text{B}$  is probably<sup>10</sup>  ${}^{11}\text{B}^*(14.33)$  whose  $J^\pi = \frac{5}{2}^{(+)}, (\frac{3}{2}^-)$ ; the former is consistent with  $L=1$ , the latter with  $L=0$  in the formation of  ${}^{11}\text{Be}(1.78)$  in the  $(t, p)$  reaction. No information on the  $J^\pi$  of the other states shown in Table II is available nor is there information from the analog region in  ${}^{11}\text{B}$ .

A distorted-wave Born-approximation (DWBA) analysis of the angular distributions determined in this reaction has been carried out with the parameters given in Table III. The ground state dis-

tribution is well fitted by  $L=1$  assuming that the transferred pair of neutrons was  $(p_{3/2}, s_{1/2})$ :  $\epsilon = 6.6 \times 10^{-3}$ . The distribution to  ${}^{11}\text{Be}^*(0.32)$  is poorly fitted by  $L=2$ , assuming  $(p_{3/2}, p_{1/2})$  transfer. The  ${}^{11}\text{Be}^*(3.94)$  angular distribution is well reproduced by  $L=0$  assuming  $(d_{5/2})^2$  transfer, and the optical model 2 (OM2) parameters (see Sec. II H.) We suggest that  ${}^{11}\text{B}^*(3.88)$  involves  $L \geq 3$  (See Sec. II B). The higher states are so unbound that analysis of the distributions by DWUCK would not be appropriate.

#### E. ${}^{10}\text{B}(t, p) {}^{12}\text{B}$

There exists a substantial body of information about the level structure of  ${}^{12}\text{B}$ : see Table IV and Refs. 10 and 11. Figure 8 shows a typical spectrum, and the parameters we obtained for the states of  ${}^{12}\text{B}$  are shown in Table IV. Angular distributions of protons have been measured at  $E_t = 10$  MeV by Middleton and Pullen<sup>2</sup>; Fig. 9 shows the distributions we obtained at  $E_t = 23$  MeV.

A DWBA analysis of the angular distributions shown in Fig. 9 is consistent with the  $L=2, 2, 1, 3, 4,$  and  $2$  assignments previously derived for  ${}^{12}\text{B}^*(0, 0.95, 1.67, 2.62, 2.72, 3.76)$ , using the OM2 parameters listed in Sec. II D.

#### F. ${}^{11}\text{B}(t, p) {}^{13}\text{B}$

A number of states with  $E_x < 8.7$  MeV have been observed<sup>12</sup>: The information stems primarily from the work of Wyborny<sup>13</sup> using the  ${}^7\text{Li}({}^7\text{Li}, p)$  reaction and of Middleton and Pullen<sup>2</sup> on the  $(t, p)$  reaction. The parameters of the states are displayed in Table V as are our results derived from

TABLE IV. States of  $^{12}\text{B}$ .

Group No. <sup>b</sup>	Present results				Previous results <sup>a</sup>			
	$E_x$ (MeV $\pm$ keV)	$\Gamma_{\text{c.m.}}$ (keV)	$I_{\text{c.m.}}$ <sup>c</sup>	$L$	$E_x$ (MeV $\pm$ keV)	$J^\pi$	$\Gamma_{\text{c.m.}}$ (keV)	$L$ <sup>d</sup>
0	0		$\equiv 1$	$2^e$	0	$1^+$		2
1	$0.959 \pm 20$		0.3	$2^e$	$0.9531 \pm 0.6$	$2^+$		2
2	$1.690 \pm 20$		0.5	$1^e$	$1.6737 \pm 0.6$	$2^-$		1
3	$\equiv 2.62$		0.06	$3^e$	$2.6208 \pm 1.2$	$1^-$		3
4	$\equiv 2.72$		0.01	$4^e$	$2.723 \pm 11$	$0^+$		4
5	$\equiv 3.39^f$				$3.3884 \pm 1.4$	$3^-$	$(3.1 \pm 0.6) \times 10^{-3}$	1
6	$3.777 \pm 20$	$40 \pm 10$	0.3	$2^e$	$3.759 \pm 6$	$2^+$	$37 \pm 5$	2
7	f				$4.302 \pm 6$	$1^-$	$9 \pm 4$	3
					4.37	$2^-$	Broad	3
8	$4.543 \pm 20$	$86 \pm 20$	1.8		$4.521 \pm 7$	$4^-$	$110 \pm 20$	1
	g				$4.99 \pm 15$	$1^+$	$50 \pm 15$	2
9	$5.63 \pm 30$	f			$5.607 \pm 7$	$3^+$	$110 \pm 20$	0
	f				$5.725 \pm 7$	$3^-$	$60 \pm 15$	3
	g				5.8	$(1)^-$	Broad	
	h				6.6	$(1)^+$	140	
	h				6.8	$(1)^+$	Broad	
10	$\equiv 7.55$				$7.545 \pm 20$	$>3$	$\leq 14$	
	g				$7.836 \pm 20$	$>0$	$60 \pm 30$	
	g				$7.937 \pm 20$	$>0$	27	
	i				$8.1 \pm 100$		$900 \pm 200$	
11	$8.16 \pm 30$		1.1		$8.120 \pm 20$			
	j				$8.24 \pm 30$	$>1$	65	
12	$\equiv 8.38$				$8.376 \pm 20$		$40 \pm 20$	
13	$\equiv 8.58$				$8.58 \pm 30$	$>1$	75	
	g				$8.707 \pm 20$			
14	$9.07 \pm 30$	$95 \pm 20$	2.0		$9.03 \pm 20$	$>1$	120	
	g				$9.175 \pm 20$			
15	$9.44 \pm 30$		0.7		$9.43 \pm 20$		$85 \pm 30$	
16	$9.626 \pm 20$	$34 \pm 10$	4.6		$9.585 \pm 20$		$60 \pm 30$	
	g				$9.758 \pm 20$			
	g				(9.83)			
	g				$10.00 \pm 40$	$>0$	100	
	g				$10.11 \pm 40$			
17	$10.227 \pm 20$	$<25$	3.6		$10.21 \pm 30$		$50 \pm 20$	
	g				$10.435 \pm 20$		$75 \pm 40$	
18	$10.61 \pm 30$	$<30$	0.8		$10.58 \pm 20$	$>2$	$50 \pm 30$	
19	$10.91 \pm 20$	$27 \pm 10$	1.1		$10.887 \pm 20$		$40 \pm 20$	
	g				(11.08)			
	g				$11.31 \pm 30$		$130 \pm 60$	
	g				$11.59 \pm 20$		$75 \pm 25$	
20	$12.36 \pm 30$		4.8		$12.33 \pm 30$	$>2$	$100 \pm 30$	
	g				$12.710 \pm 20$	$0^+; T=2$	$(85 \pm 40)$	
21	$(13.4 \pm 100)$	Broad			$13.33 \pm 30$		$50 \pm 20$	
	g				14.7	$(2^+; T=2)$	Sharp	
	g				15.5			

<sup>a</sup> See Refs. 2, 10, and 11.

<sup>b</sup> Group number as displayed in Fig. 9.

<sup>c</sup> Relative intensities at  $\theta_{\text{lab}} = 5.5^\circ$ .

<sup>d</sup> Assuming  $J^\pi$  values shown.

<sup>e</sup> See discussion in Sec. II E.

<sup>f</sup> Observed: contaminant group(s) from  $^{16}\text{O}(t, p)^{18}\text{O}$  mixed with this state at several angles.

<sup>g</sup> Not observed.

<sup>h</sup> Probably observed but groups are very weak and mixed at many angles with  $^{18}\text{O}$  groups.

<sup>i</sup> Not observed: known width too large for group to have been observed.

<sup>j</sup> Region obscured by contaminant peaks from  $^{12}\text{C}(t, p)$  and  $^{16}\text{O}(t, p)$ .

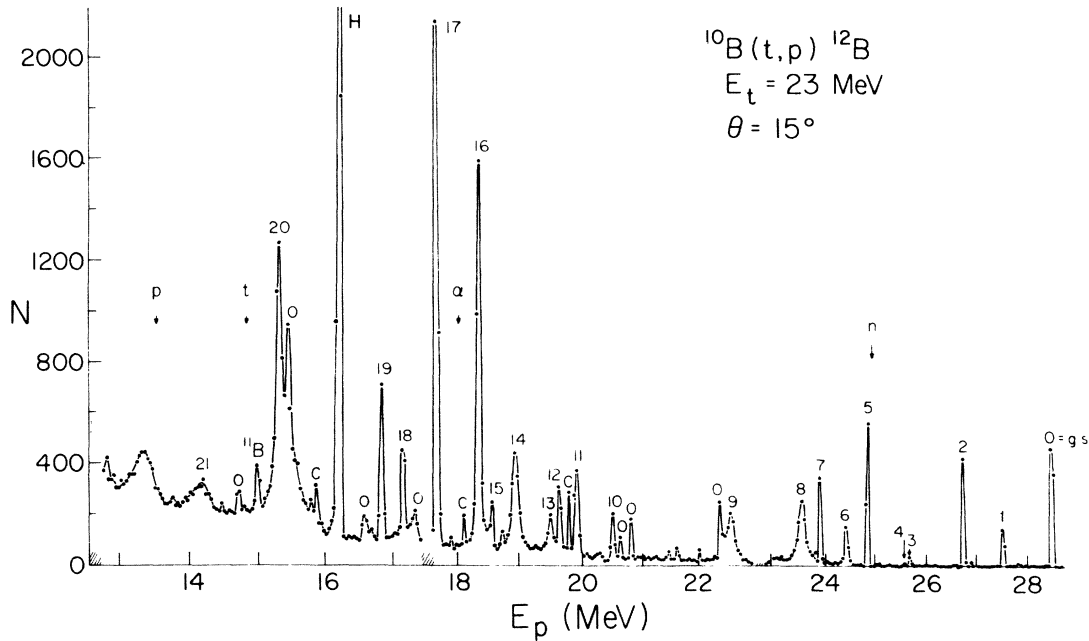


FIG. 8. Spectrum of the protons from  ${}^{10}\text{B}(t, p){}^{12}\text{B}$  at  $\theta = 15^\circ$ . The group numbers refer to the states displayed in Table IV. Groups labeled O are from the  ${}^{16}\text{O}(t, p){}^{18}\text{O}$  reaction, except for the ground state group. The group labeled H is from the  ${}^4\text{H}(t, p){}^3\text{H}$  reaction; that labeled  ${}^{11}\text{B}$  is from the  ${}^{11}\text{B}(t, p){}^{13}\text{B}$  reaction to  ${}^{13}\text{B}^*(6.17)$ . The arrows labeled  $n$ ,  $\alpha$ ,  $t$ , and  $p$  occur at the binding energies for these particles in  ${}^{12}\text{B}$ . See also the caption to Fig. 1.

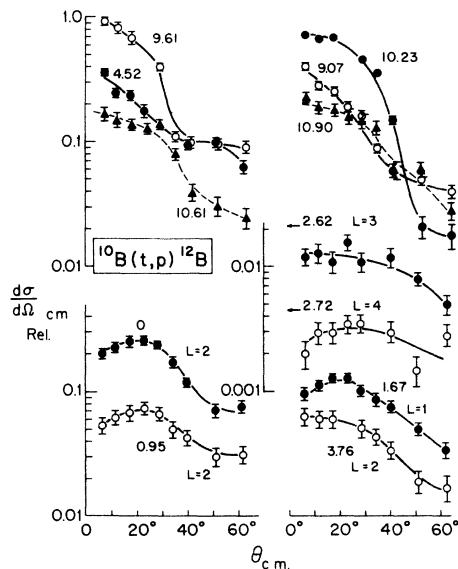


FIG. 9. Angular distributions of the protons to  ${}^{12}\text{B}^*(0, 0.95, 1.67, 2.62, 2.72, 3.76, 4.52, 9.07, 9.61, 10.23, 10.90)$ . See also the caption to Fig. 4.

spectra such as the one shown in Fig. 10 and from the angular distributions presented in Fig. 11. We report four new states of  ${}^{13}\text{B}$  with  $9.4 < E_x < 12$  MeV: see Table V. In addition, DWBA calculations confirm  $L=0$  for  ${}^{13}\text{B}(0)$  (see also Sec. IIH.)

The excited states with  $E_x < 5.1$  MeV have been assigned  $J^\pi$  based on  $L$  assignments of 1 or 2 derived from PWBA analysis of angular distributions by Middleton and Pullen.<sup>2</sup> We find no convincing correspondence between the angular distributions we observe for these states and the  $L=1$  and  $L=2$  curves derived from DWBA using the parameters discussed in Sec. IID. We observe further that Middleton and Pullen<sup>2</sup> assigned  $L=1$  to the groups to  ${}^{13}\text{B}^*(3.48, 3.68)$  and  $L=2$  to  ${}^{13}\text{B}^*(3.53, 3.71, 4.13)$  whereas our experimental distributions are closely the same for  ${}^{13}\text{B}^*(3.48, 3.53)$  and for  ${}^{13}\text{B}^*(3.68, 3.71)$  suggesting that the same  $L$  value is involved for each of the two members of these closely spaced levels. Most of the other angular distributions shown in Fig. 11 involve highly unbound states which are not amenable to analysis at this time. One might suggest, however, that  ${}^{13}\text{B}^*(6.93)$  in-

TABLE V. States of  $^{13}\text{B}$ .

Group No. <sup>b</sup>	Present results				Previous results <sup>a</sup>			
	$E_x$ (MeV $\pm$ keV)	$\Gamma_{c.m.}$ (keV)	$I_{c.m.}$ <sup>c</sup>	$L$	$E_x$ (MeV $\pm$ keV)	$J^\pi$	$\Gamma_{c.m.}$ (keV)	$L$ <sup>d</sup>
0	0		$\equiv 1$	$0^e$	0	$\frac{3}{2}^-$		0
1	$3.482 \pm 10$		0.1	e	$3.483 \pm 5$	$(\frac{1}{2}, \frac{3}{2}, \frac{5}{2})^+$		1
2	$3.531 \pm 10$		0.3	e	$3.5347 \pm 3.5$	$(\frac{1}{2}, \frac{3}{2}, \frac{7}{2})^-$		2
3	$3.681 \pm 10$		0.6	e	$3.681 \pm 5$	$(\frac{1}{2}, \frac{3}{2}, \frac{5}{2})^+$		1
4	$3.715 \pm 10$		0.4	e	$3.712 \pm 5$	$(\frac{1}{2}, \frac{3}{2}, \frac{7}{2})^-$		2
5	$4.128 \pm 10$		1.6		$4.131 \pm 5$	$(\frac{1}{2}, \frac{3}{2}, \frac{7}{2})^-$		2
6	$4.834 \pm 10$		0.05		$4.827 \pm 7$			
7	$5.023 \pm 10$		0.3		$5.033 \pm 8$	$(\frac{1}{2}, \frac{3}{2}, \frac{5}{2})^+$		1 <sup>f</sup>
8	$5.106 \pm 10$	$60 \pm 10$	0.1					
9	$5.393 \pm 10$	$10 \pm 10$	1.1		$5.390 \pm 7$		$15 \pm 5$	
	g				$5.557 \pm 8$			
10	$6.164 \pm 10$		1.6		$6.169 \pm 8$			
11	$6.434 \pm 10$	$36 \pm 5$	1.5		$6.419 \pm 8$			
12	$6.932 \pm 10$	$55 \pm 15$	0.2	$\geq 4^e$	$6.939 \pm 15$			
	g				$7.516 \pm 8$			
	g				$7.859 \pm 20$			
13	$8.138 \pm 10$	$100 \pm 15$	1.2		$8.129 \pm 10$			
14	$8.684 \pm 10$	$89 \pm 20$	0.5		$8.682 \pm 9$			
15	$9.44 \pm 30$	$81 \pm 25$	0.1					
16	$10.22 \pm 20$	$210 \pm 20$	2.1					
17	$10.89 \pm 20$							
18	(11.80)							

<sup>a</sup> See Refs. 2 and 13. See also Ref. 12.

<sup>b</sup> Group number as displayed in Fig. 11.

<sup>c</sup> Relative intensities at  $\theta_{lab} = 10^\circ$ .

<sup>d</sup> Reference 2.

<sup>e</sup> See discussion in Sec. II F.

<sup>f</sup> But see group 8 which was unresolved in the work of Ref. 2.

<sup>g</sup> Not observed.

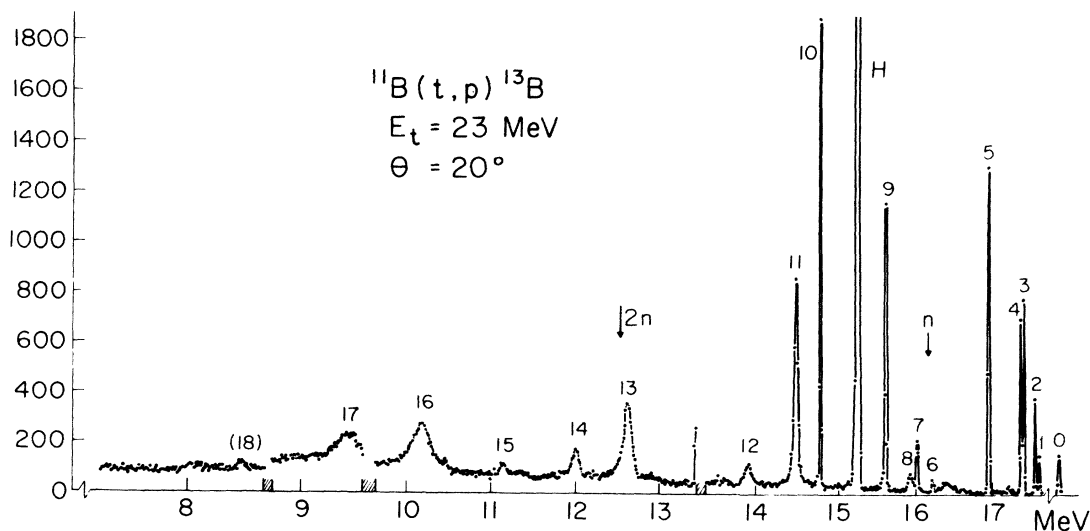


FIG. 10. Spectrum of the protons from  $^{11}\text{B}(t,p)^{13}\text{B}$  at  $\theta = 20^\circ$ . The group numbers refer to the states displayed in Table V. See also the captions to Figs. 1 and 8.

TABLE VI. States of  ${}^{14}\text{C}$ .

Group No. <sup>b</sup>	Present results		Previous results			$L$ <sup>c</sup>
	$E_x$ (MeV $\pm$ keV)	$(d\sigma/d\Omega)_{\text{c.m.}}^{\text{max}}$ <sup>a</sup> (mb/sr)	$E_x$ (MeV $\pm$ keV)	$J^\pi$	$\Gamma_{\text{c.m.}}$ <sup>c</sup> (keV)	
0	0	1.26 $\pm$ 0.05	0	0 <sup>+</sup>		0
1	6.099 $\pm$ 10	0.36 $\pm$ 0.01	6.0942 $\pm$ 1.6	1 <sup>-</sup>		1
2	6.589 $\pm$ 10	0.23 $\pm$ 0.01	6.5898 $\pm$ 1.6	0 <sup>+</sup>		0
3	6.731 $\pm$ 10	1.75 $\pm$ 0.05	6.7282 $\pm$ 1.3	3 <sup>-</sup>		3
4	6.899 $\pm$ 10	0.014 $\pm$ 0.005	6.9023 $\pm$ 1.8	0 <sup>-</sup>		
5	7.017 $\pm$ 10	2.13 $\pm$ 0.05	7.0120 $\pm$ 4.2	2 <sup>+</sup>		2
6	7.342 $\pm$ 10	0.071 $\pm$ 0.005	7.3414 $\pm$ 3.1	2 <sup>-</sup>		
7	8.315 $\pm$ 10	1.22 $\pm$ 0.03	8.3183 $\pm$ 0.9	2 <sup>+</sup>	3.4 $\pm$ 0.6	2
8	9.80 $\pm$ 20	d	9.799 $\pm$ 7	(3, 1)	45 $\pm$ 12	
9	10.419 $\pm$ 20	0.98 $\pm$ 0.04	10.437 $\pm$ 9	(2 <sup>+</sup> , 3)	16	
10	10.492 $\pm$ 20	0.13 $\pm$ 0.02	10.509 $\pm$ 13	(4 <sup>+</sup> )	26 $\pm$ 8	(4)
11	10.730 $\pm$ 20	3.53 $\pm$ 0.05	10.743 $\pm$ 5		20 $\pm$ 7	
	e		11.306 $\pm$ 15	1 <sup>(-)</sup>	46 $\pm$ 12	
12	11.377 $\pm$ 20	0.055 $\pm$ 0.010	11.397 $\pm$ 15	(2 <sup>+</sup> , 3)	22 $\pm$ 7	
13	11.647 $\pm$ 30	0.137 $\pm$ 0.020	11.667 $\pm$ 15	(5 <sup>-</sup> )	20 $\pm$ 7	(5)
	d		11.740 $\pm$ 20			
	e		11.9 $\pm$ 300		950 $\pm$ 300	
	e		12.589 $\pm$ 16		105 $\pm$ 15	
14	12.849 $\pm$ 20	0.35 $\pm$ 0.03	12.860 $\pm$ 14	(4, 5)	30 $\pm$ 10	
15	12.945 $\pm$ 30	0.47 $\pm$ 0.03	12.964 $\pm$ 14	(3, 4)	30 $\pm$ 10	

<sup>a</sup> Uncertainties shown are statistical only. Absolute values are estimated to be  $\pm 30\%$ .

<sup>b</sup> Group number as displayed in Fig. 13.

<sup>c</sup> See Ref. 12.  $L$  values derived from  $J^\pi$  shown, except when indicated otherwise.

<sup>d</sup> Very weak at all angles.

<sup>e</sup> Not observed.

volves  $L \geq 4$ , as discussed earlier (see, e.g., Sec. II B).

### G. ${}^{12}\text{C}(t, p){}^{14}\text{C}$

States in  ${}^{14}\text{C}$  with  $E_x < 13$  MeV are displayed in Table VI: See Refs. 12 and 14. Table VI also shows our results derived from spectra such as the one shown in Fig. 12 and from the angular distributions of Fig. 13. Data were obtained using methane gas to provide accurate values for the absolute cross sections.

The DWBA calculations using the OM1 parameters discussed in Sec. II D reproduce fairly well the angular distributions for  $L=0$  transitions to

${}^{14}\text{C}^*(0, 6.09)$  and the  $L=2$  distributions to  ${}^{14}\text{C}^*(7.01)$ ,  $8.32$ ). However, the theoretical curve for  $L=1$  does not fit the distribution to  ${}^{14}\text{C}^*(6.09)$  whose  $J^\pi$  is well known to be  $1^-$ . We note that the cross sections for populating  ${}^{14}\text{C}^*(6.90, 7.34)$  are relatively small and the distributions are quite featureless: This is expected since these two states are known to have  $J^\pi=0^-$  and  $2^-$  and they cannot be reached by a simple double stripping mechanism. The other states shown in Fig. 13 are highly unbound and not easily analyzed using DWBA techniques. However, the similarities in the angular distributions to  ${}^{14}\text{C}^*(12.85, 12.95)$  suggest that the same  $L$  is involved in both cases (see also Table VI).

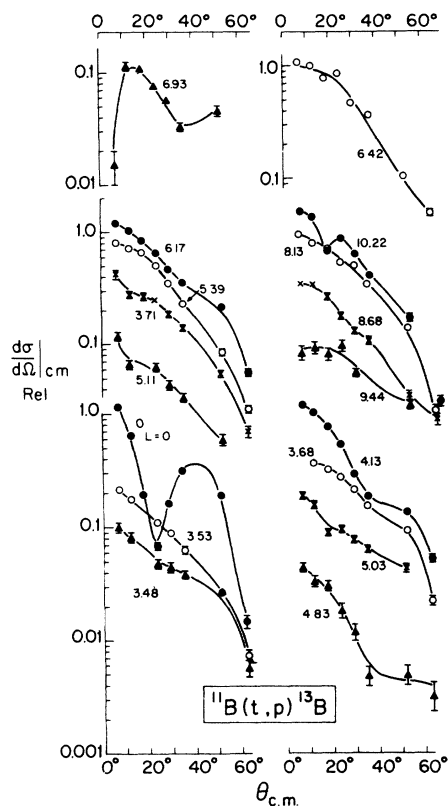


FIG. 11. Angular distributions of the protons to  $^{13}\text{B}^*(0, 3.48, 3.53, 3.68, 3.71, 4.13, 4.83, 5.03, 5.11, 5.39, 6.17, 6.42, 6.93, 8.13, 8.68, 9.44, 10.22)$ . See also the caption to Fig. 4.

#### H. $L = 0$ angular distributions

Our attempts to fit angular distributions of bound or slightly unbound states which involve  $L = 1$  or 2 using the DWBA code have been only moderately successful. Fits can, of course, be obtained by arbitrarily varying parameters but no consistent results are obtained with a single set of reasonably varying parameters. Full finite range, full recoil calculations are a necessary next step in the analysis but the accuracy of the present experimental cross sections does not justify this procedure. However, in the preceding discussion we have pointed out that certain  $L$  assignments can be made by comparisons with the distributions to states of known  $J^\pi$ , in particular where large  $L$  values are involved. Further, we are able to fit  $L = 0$  distributions in a consistent way with the DWBA formalism, except in the cases of  $^6\text{He}_{g.s.}$  and  $^8\text{Li}_{0.95}^*$ : Fig. 14 shows the comparison of the experimental distributions to  $^{13}\text{B}_{g.s.}$ ,  $^{14}\text{C}_{g.s.}$ , and  $^{14}\text{C}_{6.59}^*$ . The success in these cases, all of which are characterized by a strong diffraction minimum, leads us to assign  $L = 0$  to the transitions to  $^9\text{Li}_{g.s.}$  and  $^{11}\text{Be}_{3.94}^*$ .

We acknowledge with thanks the aid of the staff of the LASL tandem. We are particularly grateful to Stuart Orbesen for his assistance during the experiment and to Dr. J. D. Garrett for his many suggestions in the analysis of the data. We are indebted also to Marie Barnett and Rena Wardaski at Penn, to Dorothy Squires, Syrena Tucker, and

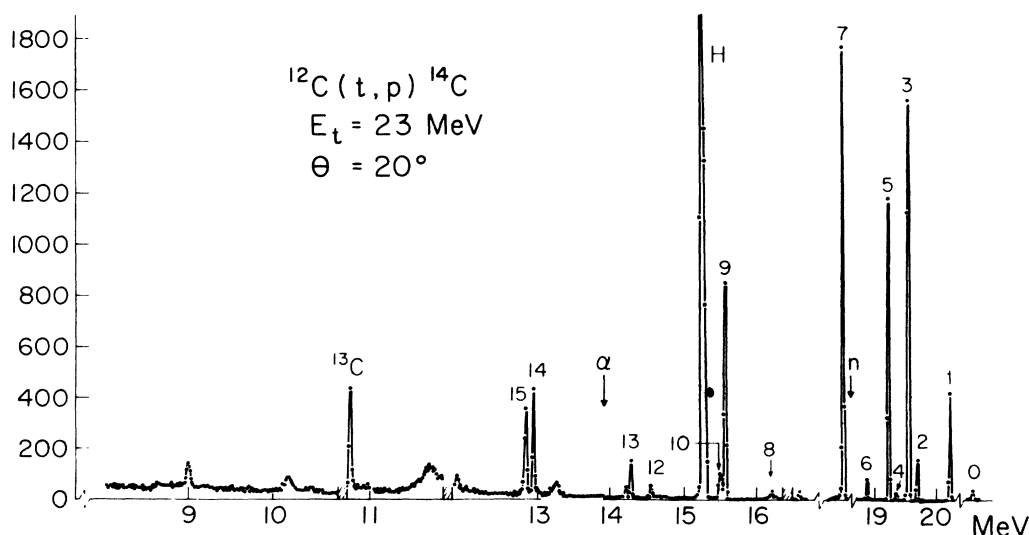


FIG. 12. Spectrum of the protons from  $^{12}\text{C}(t,p)^{14}\text{C}$  at  $\theta = 20^\circ$ . The group numbers refer to the states displayed in Table VI. See also the captions to Figs. 1 and 8.

